# Supporting Information

# Halochromic Oxazolidine Nanofibers as Portable Smart Chemosensor for Dual-Mode Colorimetric and Fluorimetric Detection of Food Spoilage: Investigation the Solid-State pH-Responsivity in Polar Microenvironments

**Bahareh Razavi [a], Babak Karimi* [a,b]**

[a] Department of Chemistry, Institute for Advanced Studies in Basic Sciences (IASBS), Zanjan, 45137-66731, Iran

[b]Research Center for Basic Sciences & Modern Technologies (RBST), Institute for Advanced Studies in Basic Sciences (IASBS), Zanjan, 45137-66731, Iran

* Correspondence concerning this article should be addressed to Babak Karimi: karimi@iasbs.ac.ir

## 1. Synthesis of oxazolidine derivatives

The oxazolidine with hydroxyl and tertiary amine was synthesized and typical procedure are presented in Scheme S1.


**Scheme S1.** Typical procedures for the synthesis is of oxazolidine derivatives from different indolium salts and aldehyde compounds

## 2. Characterization

Characterization of the chemical structure of OX-OH, OX-$NMe_2$, PM-NPs, PMDM-NPs, PMHM-NPs, and PMSO-NPs was carried out by proton nuclear magnetic resonance ($^1$HNMR) spectroscopy using a Bruker DPX 400 MHz apparatus in DMSO solvent for fluorescence dye and $CDCl_3$ solvent for NPs. Identification of different functional groups on polymer nanoparticles was carried out by using an ATIR BRUKER-IFS48 spectrophotometer (Germany). Samples were prepared after drying the latex particles at room temperature, washing with water several times, drying at 50 °C, and dispersing in KBr pellets. The measurement of particle size and its distribution was performed by using ZETASIZER NANO ZSP dynamic light scattering (DLS, Malvern,

United Kingdom) at 25 °C. For this purpose, the initial polymer nanoparticle latex samples were diluted in DI water with a concentration of about 1 mg. $mL^{-1}$. The quality of the prepared polymer chains was assessed through High Performance Liquid Chromatograph (GPC) analysis using Smartline 1000-Knauer with flow rate 1 $ml.min^{-1}$. The field emission scanning electron microscopy (FESEM) micrographs were taken by a Tescan Mira III (Czech Republic). A drop of diluted latex samples was placed on the sample holder and dried in a vacuum at 25°C. To investigate the morphology of the nanofiber, surface a layer of gold was deposited under flushing with argon by using EMITECH K450x sputter-coating (UK). The nitrogen adsorption-desorption isotherms were obtained using a Belsorp (BELMAX, Japan) analyzer at 77 K. All the samples were first degassed at 353 K for 10 h before the measurements. Specific surface area of the materials was determined from the linear part of the BET plot at the relative pressure range (P/P0) of 0.05-0.15. The fluorescence intensity of samples was investigated by using OPTIC-B-500 TIFL (Italy). The surface topology of oxazolidine nanofibers was demonstrated by Atomic Force Microscope using a BRISK, (Ara researchco/Iran). Investigation of the solid fluorescence emission for nanofibers was carried out by using the Cary Eclipse fluorescence spectrophotometer (Varian America), To evaluate fluorescence properties, the excitation was done by a UV lamp (365 nm, 50 $W/m^2$) and CAMAG 12VDC/VAC (50/60 Hz, 14VA, Switzerland). To investigate hydrophilicity and hydrophobicity of the fibrous tissues, the contact angle of the water droplet on the paper surface was measured using a KRUSS G10 system (Germany) at room temperature and 25% relative humidity. The surface roughness of the fluorescence nanofibers was evaluated by using an Optical 3D Profilometer (Fathoptics/Asia,Iran). An electrospinning instrument CO881007NYI (Asia Nanostructure) was used to prepare the photo-responsive nanofibers. The syringe rate of 0.7–0.9 $mL.h^{-1}$, a fixed electrical voltage of 16–19 kV, and a tip-to-collector

distance of 20 cm were used in the electrospinning experiments. Also, the source of the visible light was a common LED lamp (8 $W/m^2$). The photography was conducted by using an iPhone camera with the model 13 Pro, in which the fluorescent images were taken under UV light.

### 3. Characterization of chemical structure by $^1$HNMR and ATR-FTIR spectroscopy

The successfully synthesize of oxazolidine derivatives were confirm by $^1$HNMR analysis. The condensation reaction between indole salt and aldehyde compounds, formed the unsaturated alkane bond that as shown in Figure S1, as a doublet signals around in 7 ppm, and 8.1 ppm for D and E respectively. In the OX-NM sample, the peak about 3.3 ppm indicate the methyl groups, and in the OX-OH sample, peaks around 10.7 ppm refers to aromatic hydroxyl group. For polymer nanoparticles, the characteristic peaks for samples are illustrated and labeled in the Figure S2.

As shown in Figure S3, in ATR-FTIR spectra, peak about 1650-1750 $cm^{-1}$, refers to stretching vibrational motion of the carbonyl ester group in all samples. The peak in 3300-3700 $cm^{-1}$, attributed to stretching vibration of hydroxyl group in the PMHM-NPs sample. The peak at about 3300-3800 $cm^{-1}$, illustrated to amide functional group in PMSO-NPs.

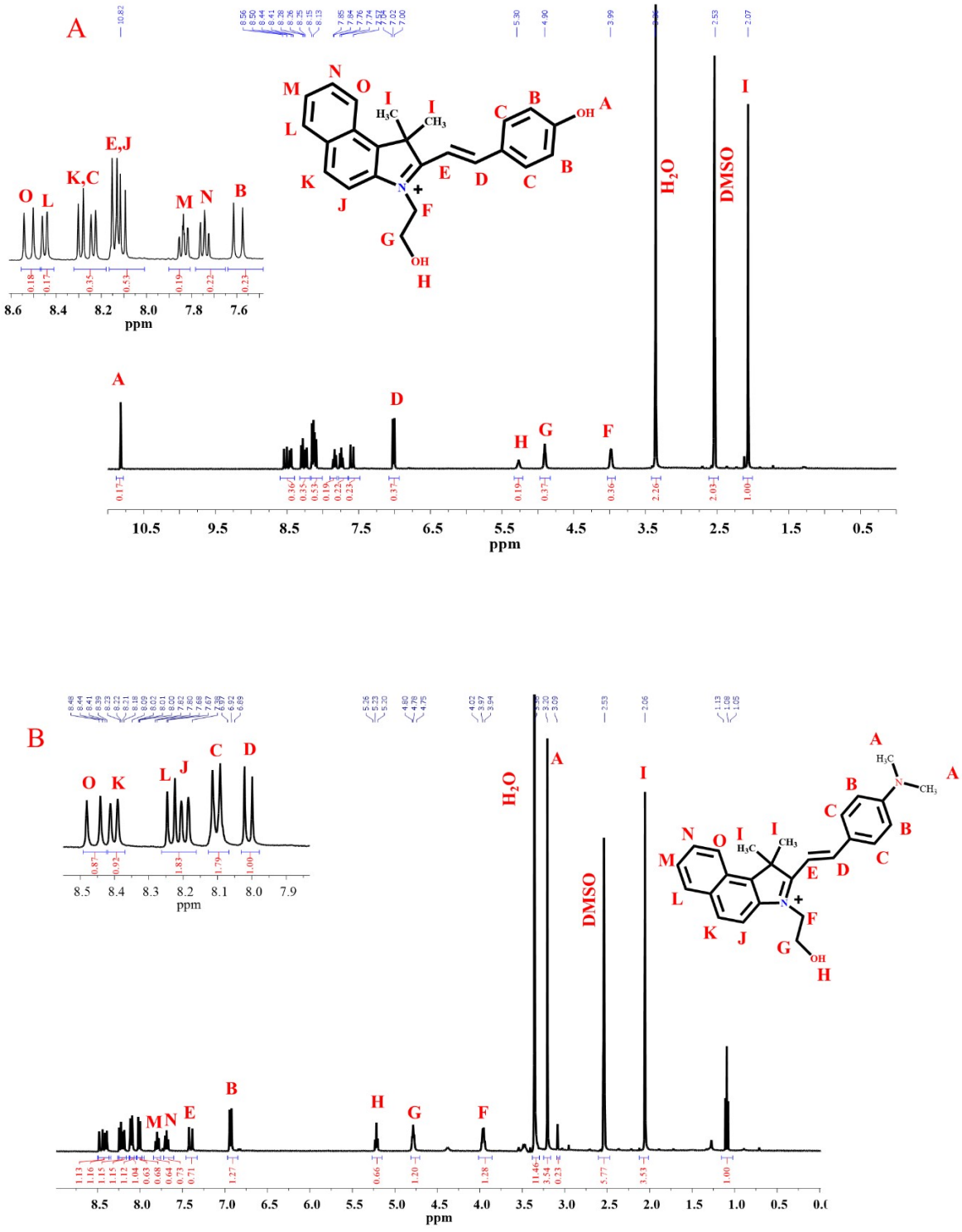


**Figure S1.** [1]HNMR spectra of (A) OX-OH and (B) OX-NM in DMSO

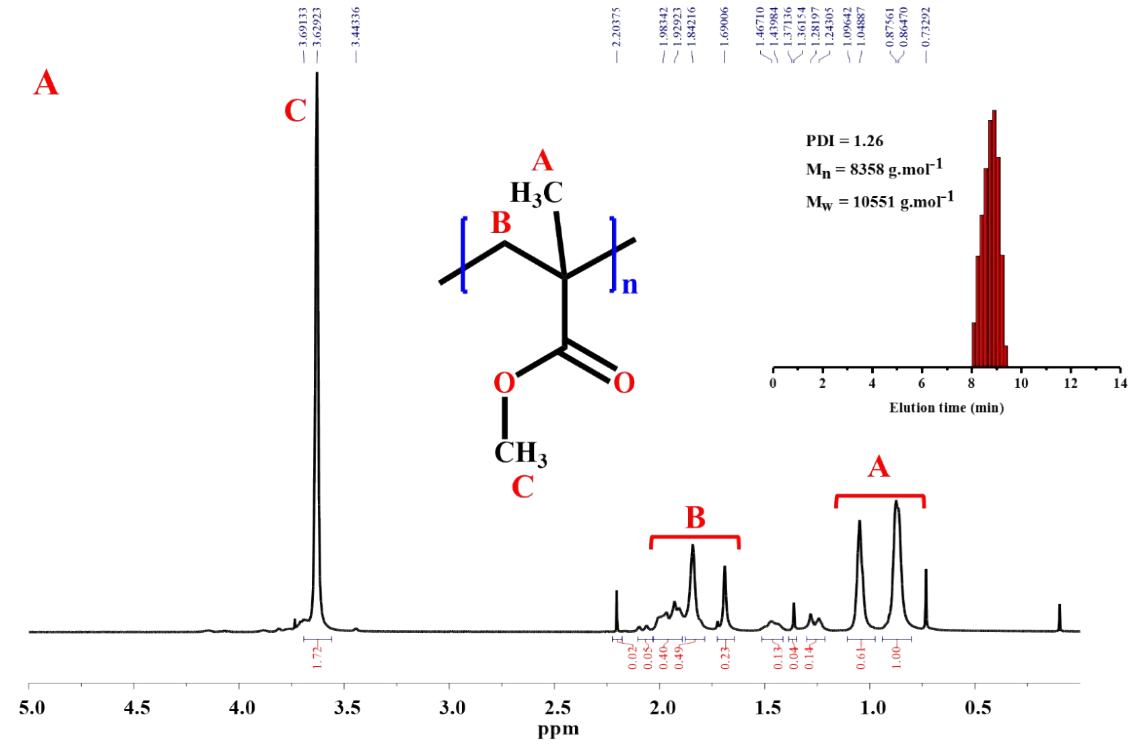
A
C
A
B
n
O
O
CH3
C
PDI = 1.26
Mn = 8358 g.mol-1
MW = 10551 g.mol-1
Elution time (min)
B
A
ppm

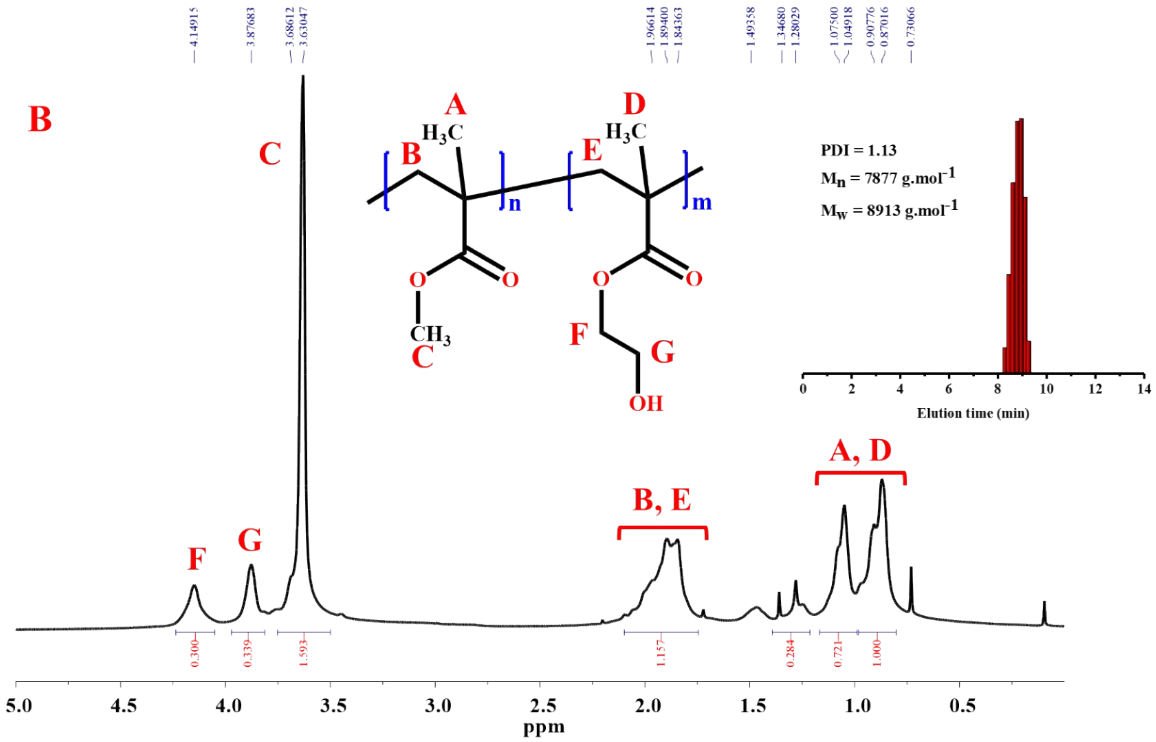
B
C
A
H3C
B
n
D
H3C
E
m
O
O
CH3
C
F
G
OH
PDI = 1.13
Mn = 7877 g.mol-1
MW = 8913 g.mol-1
Elution time (min)
F
G
B, E
A, D
ppm

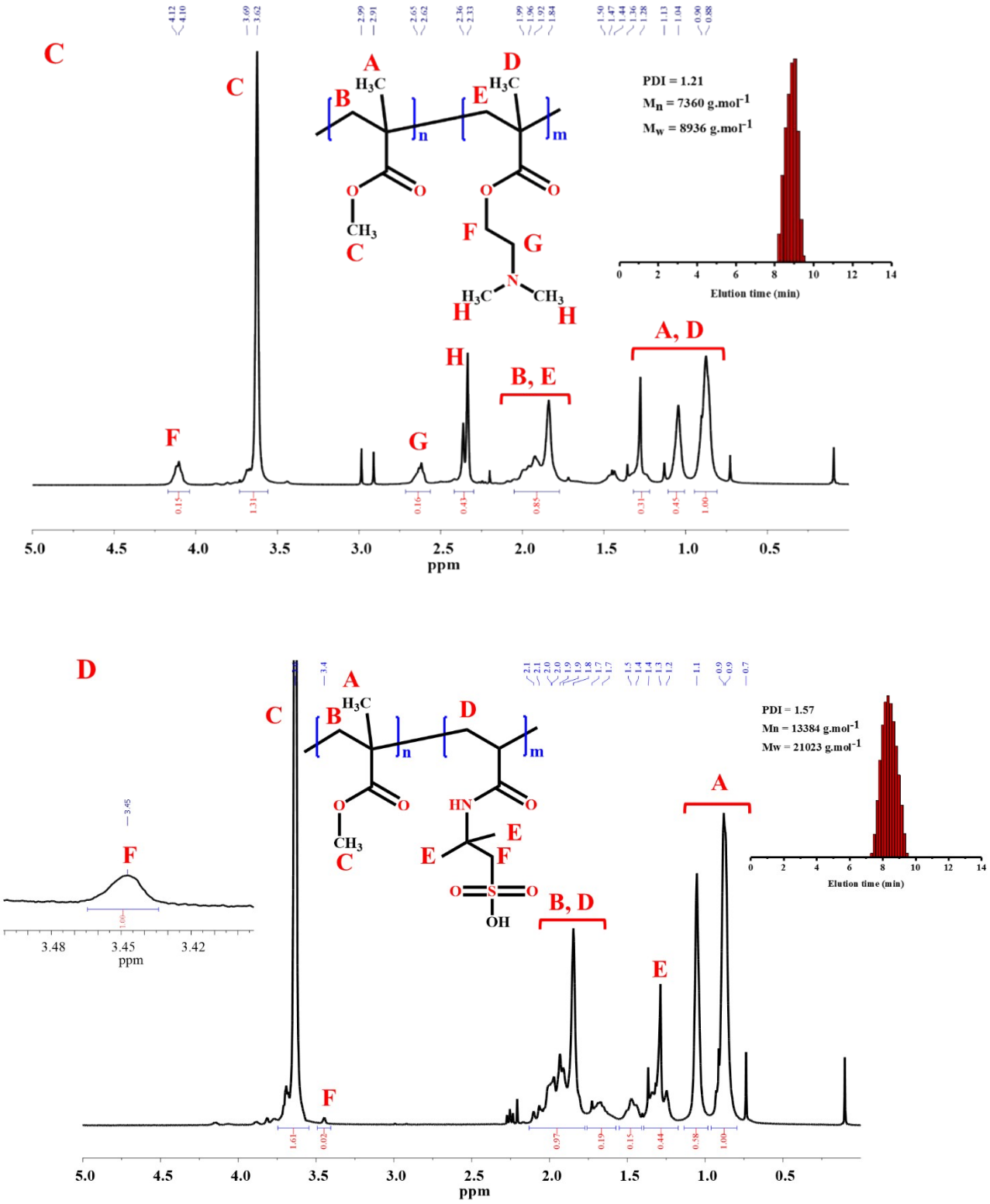


**Figure S2.** [1]HNMR spectra of (A) PM-NPs, (B) PMHM-NPs, (C) PMDM-NPs, and (D) PMSO-NPs in $CDCl_3$

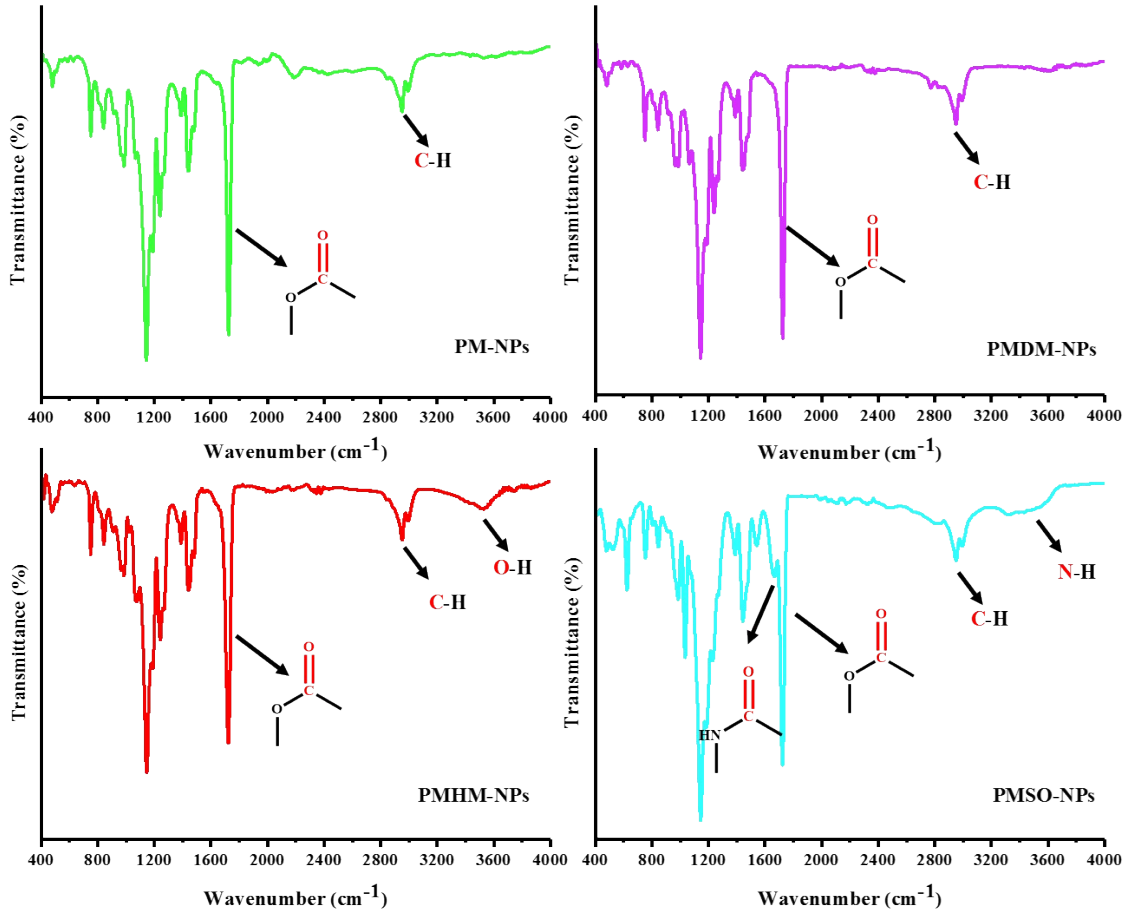


**Figure S3.** ATR-FTIR spectra of polymer nanoparticles

## 4. Determination of molecular weight by $^{1}$HNMR spectroscopy

The degree of polymerization (DP) and molecular weight (MW) of the samples were determined by integrating the peak areas of hydrogen A (representing the chain-end group), hydrogen C (corresponding to the repeating units of PMMA), and hydrogen E (associated with the repeating units of DMAEMA), (Figure S4) using Equations 1–4.

$$DP=(C/3)/(A/2) \quad \text{(Equation 1)}$$

$$MW=DP\times 100.12 \text{ (molecular weight of MMA monomer)} \quad \text{(Equation 2)}$$

DP=(E/2)/(A/2) (Equation 3)

MW=DP×157.21 (molecular weight of DMAEMA monomer) (Equation 4)

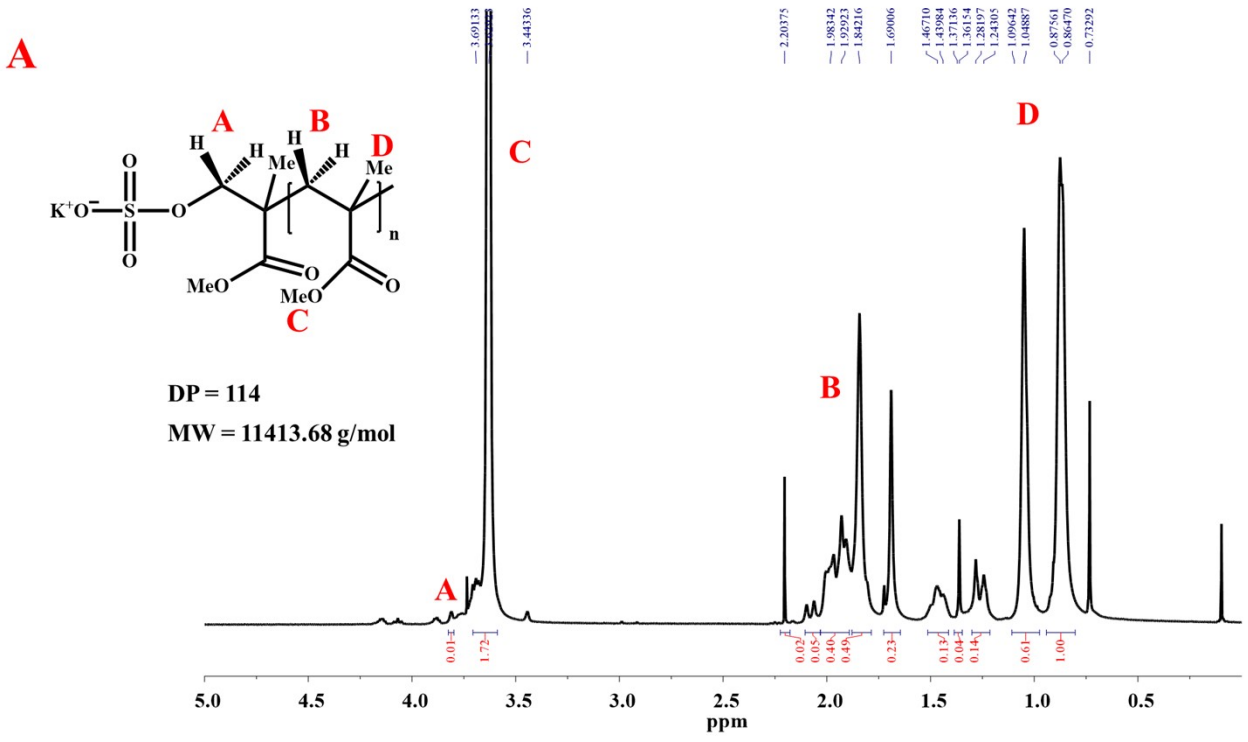

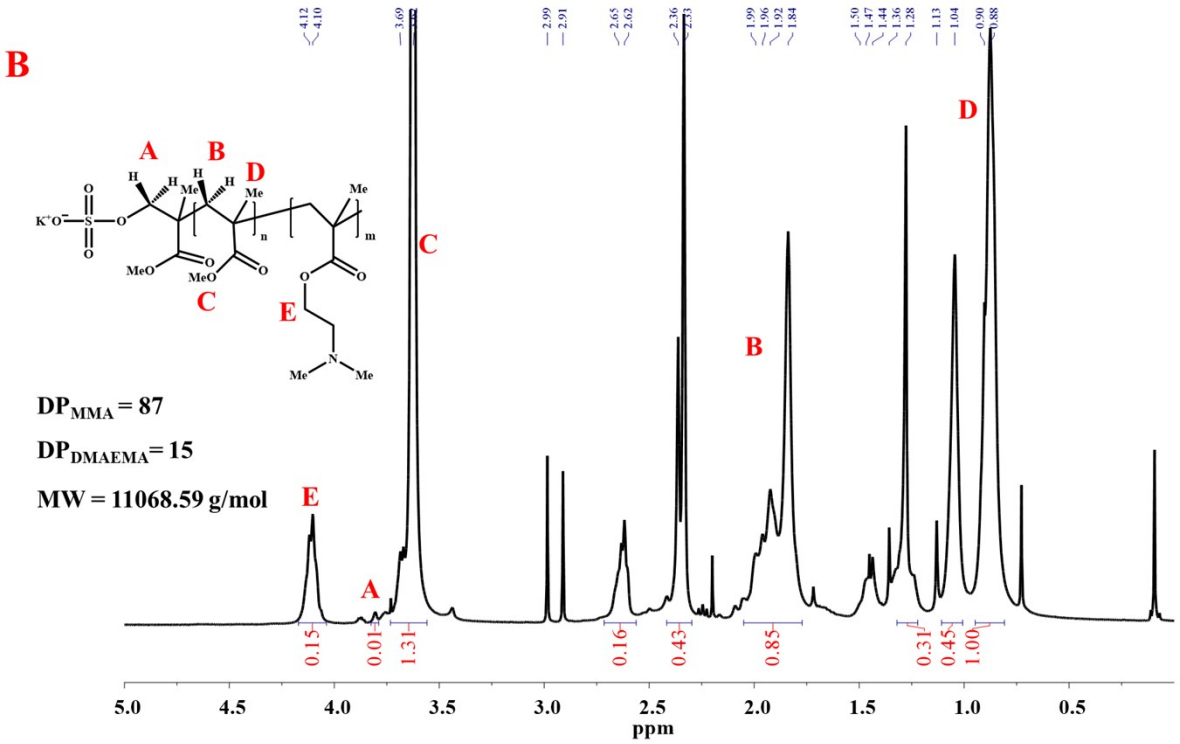


**Figure S4.** $^{1}$HNMR spectra of (A) PM-NPs, and (B) PMDM-NPs in $CDCl_3$

**Table S1. Determination of chain parameters for PM-NPs sample by $^{1}$H NMR and GPC**

| Hydrogen | Number of Hydrogens | Chemical Shift (ppm) | Integral |
|---|---|---|---|
| $H_A$ | 2 | 3.8 | 0.01 |
| $H_C$ | 3 | 3.5-3.75 | 1.72 |

| Chain Parameters | Value |
|---|---|
| $DP_{MMA}$ ($^{1}$H NMR) | 114 |
| MW($^{1}$H NMR) | 11413.68 g/mol |
| $M_w$(GPC) | 10551 g/mol |
| $M_n$(GPC) | 8358 g/mol |
| PDI | 1.26 |

**Table S2. Determination of chain parameters for PMDM-NPs sample by $^1$H NMR and GPC**

| Hydrogen | Number of Hydrogens | Chemical Shift (ppm) | Integral |
|---|---|---|---|
| $H_A$ | 2 | 3.8 | 0.01 |
| $H_C$ | 3 | 3.5-3.75 | 1.31 |
| $H_E$ | 2 | 4-4.25 | 0.15 |

| Chain Parameters | Value |
|---|---|
| $DP_{MMA}$ ($^1$H NMR) | 87 |
| $DP_{DMAEMA}$ ($^1$H NMR) | 15 |
| MW($^1$H NMR) | 11068.59 g/mol |
| $M_W$(GPC) | 8936 g/mol |
| $M_n$(GPC) | 7360 g/mol |
| PDI | 1.21 |

## 5. Investigation of the particle size and morphology of copolymer nanoparticles

One key factor in controlling the size and morphology of copolymer nanoparticles is the presence of functional groups within the copolymer structure. In this study, hydroxyl, sulfonic acid, and tertiary amine functional groups were incorporated into the copolymers, and their particle sizes were analyzed using dynamic light scattering (DLS) and field emission scanning electron microscopy (FE-SEM), as illustrated in Figures S5 and S6, respectively. Figure S5 presents the DLS curves for latex samples including various functional groups. The PM-NPs, which consist of non-functionalized PMMA nanoparticles, exhibited an average particle size of approximately 32 nm. Notably, the PMHM-NPs and PMDM-NPs displayed larger particle sizes, measuring approximately 171 nm and 142 nm, respectively, which can be attributed to the hydrophilic nature of HEMA, and DMAEMA. This hydrophilicity likely enhances water

absorption in the outer layers of particle surface, resulting in the increased particle sizes observed in PMHM-NPs, and PMDM-NPs. The smaller particle size of approximately 43 nm for PMSO-NPs can be attributed to the increased negative charge induced by the sulfonate groups. The additional negative charge enhances the repulsive interactions between the nanoparticles, resulting in a reduction in particle size. The morphology of latex samples was examined using FESEM after diluting the latex samples in water and subjecting them to 1 minute of sonication. A drop of the diluted latex was deposited on aluminum foil, allowed to dry, coated with a thin gold layer, and then analyzed. As depicted in Figure S6, the non-functionalized PMMA nanoparticles displayed a particle size of less than 40 nm, a uniform size distribution, and a well-defined spherical morphology (Figure S6A, A'). When PMMA nanoparticles were functionalized with DMAEMA (Figure S6B, B′), and HEMA (Figure S6C, C′), the particle size increased, which is consistent with the DLS results. This increase in particle size is attributed to the introduction of polar groups that enhance the polarity of PMMA chains. However, the sulfonic acid groups in hydrophilic APSA acted as co-surfactants, leading to a significant decrease in particle size (Figure S6D, D′). The primary reason for utilizing emulsion polymerization in this study is its ability to produce copolymers with a higher molecular weight. This increased molecular weight is crucial for the electrospinning process, as it significantly impacts the quality and properties of the resulting nanofibers. Therefore, all the samples are suitable for the preparation of nanofibers, with their optical properties being key in selecting the best candidate for designing smart sensors in active-intelligent food packaging.

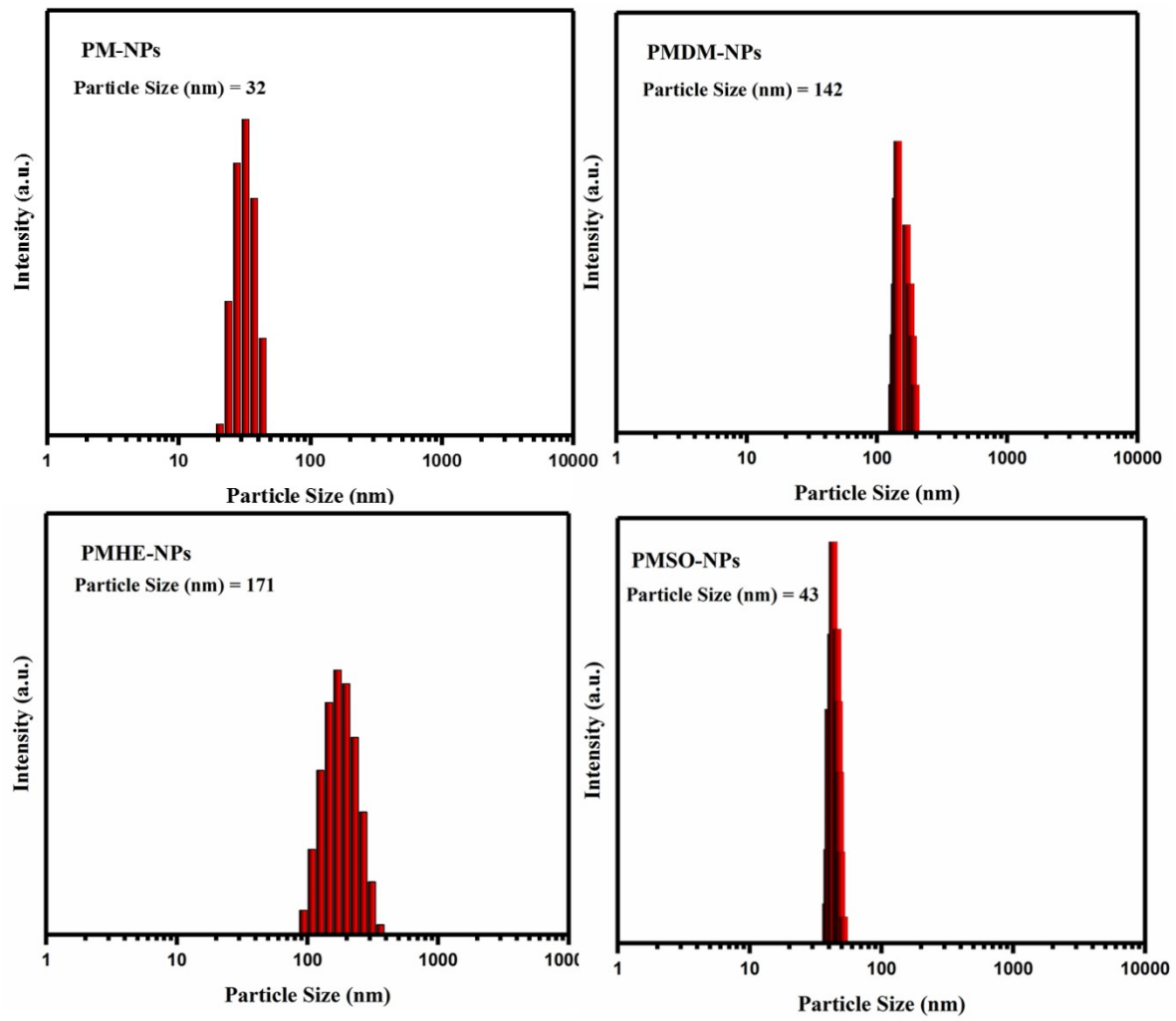


**Figure S5.** DLS analysis of polymer nanoparticles

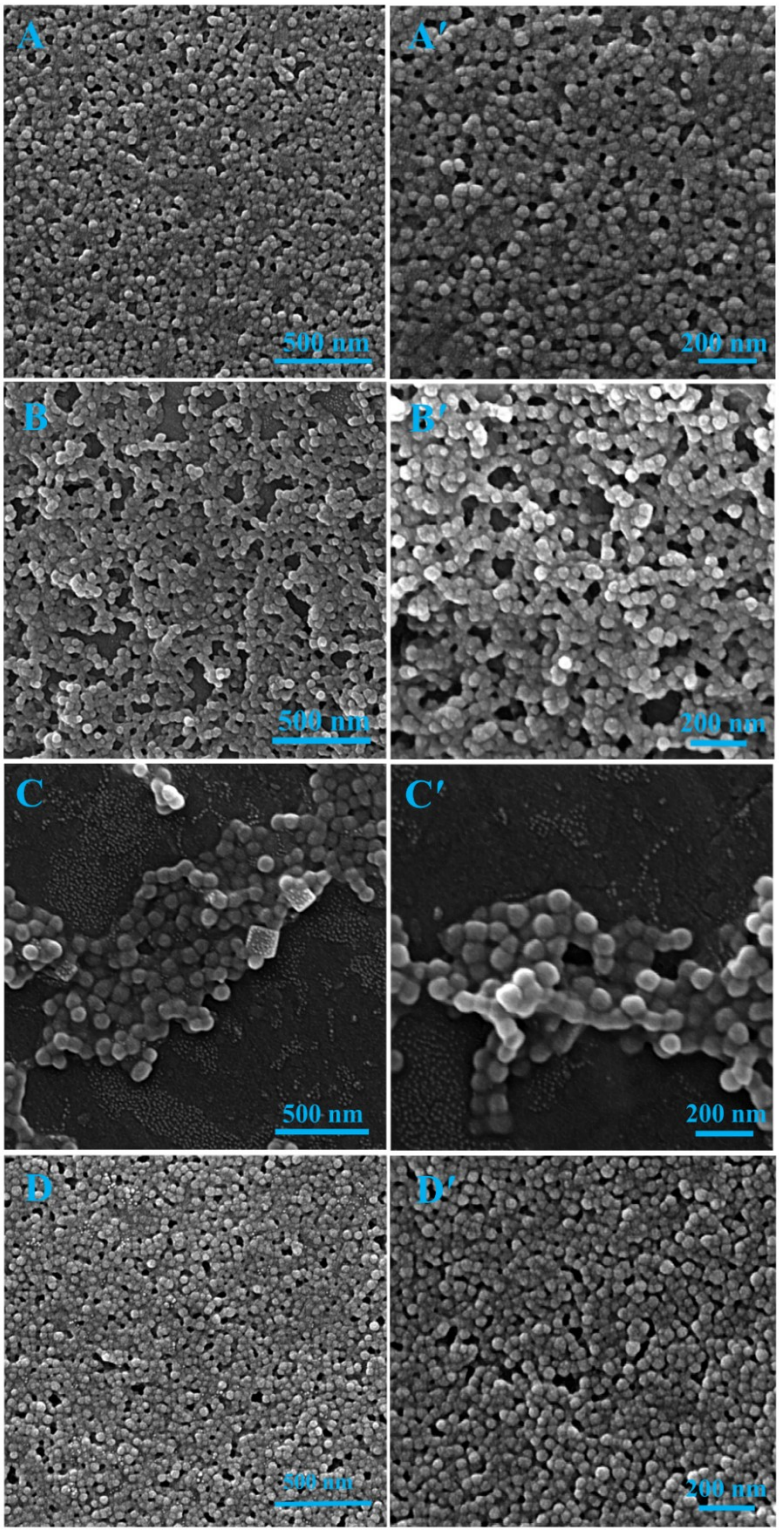


**Figure S6**. FESEM images of copolymer nanoparticles of (A, A′) PM-NPs, (B, B′) PMDM-NPs, (C, C′) PMHM-NPs, and (D, D′) PMSO-NPs

## 6. Investigation of the adsorption isotherm diagram in BET

The adsorption isotherm diagram in BET analysis provides valuable insights into the surface characteristics and porosity of materials. This diagram plots the amount of gas adsorbed on the material's surface against the relative pressure (P/P0) of the gas.

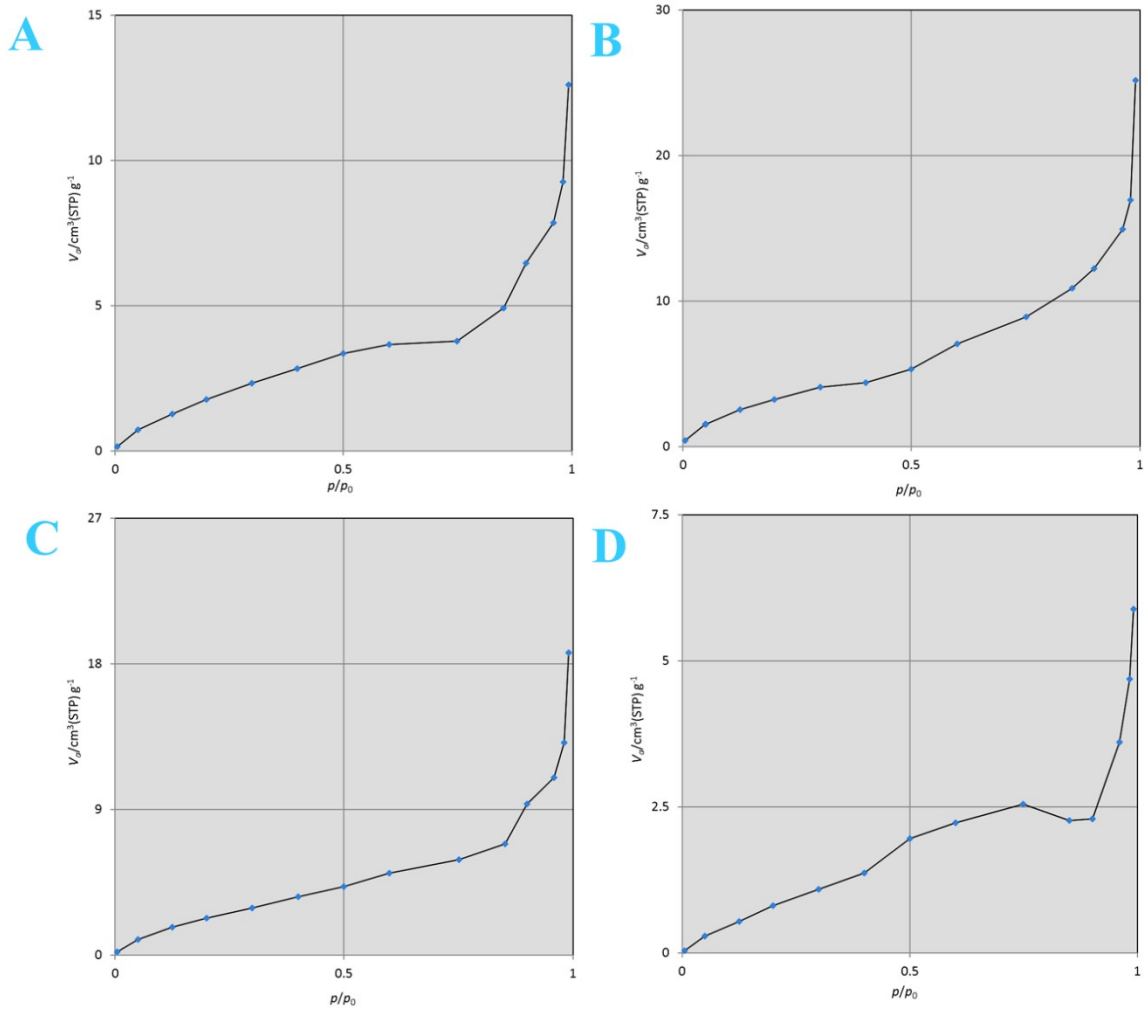


**Figure S7**. BET analysis of nitrogen adsorption isotherm curves consist of (A) PM-NFs, (B) PMHM-NFs, (C) PMDM-NPFs, and (D) PMSO-NFs

**7. Investigation of the morphology of fluorescence nanofiber by AFM analysis**

AFM analysis was used and results of images are presented on Figure S8, to confirm the similar morphology after doping oxazolidine dyes into the nanofiber matrix.

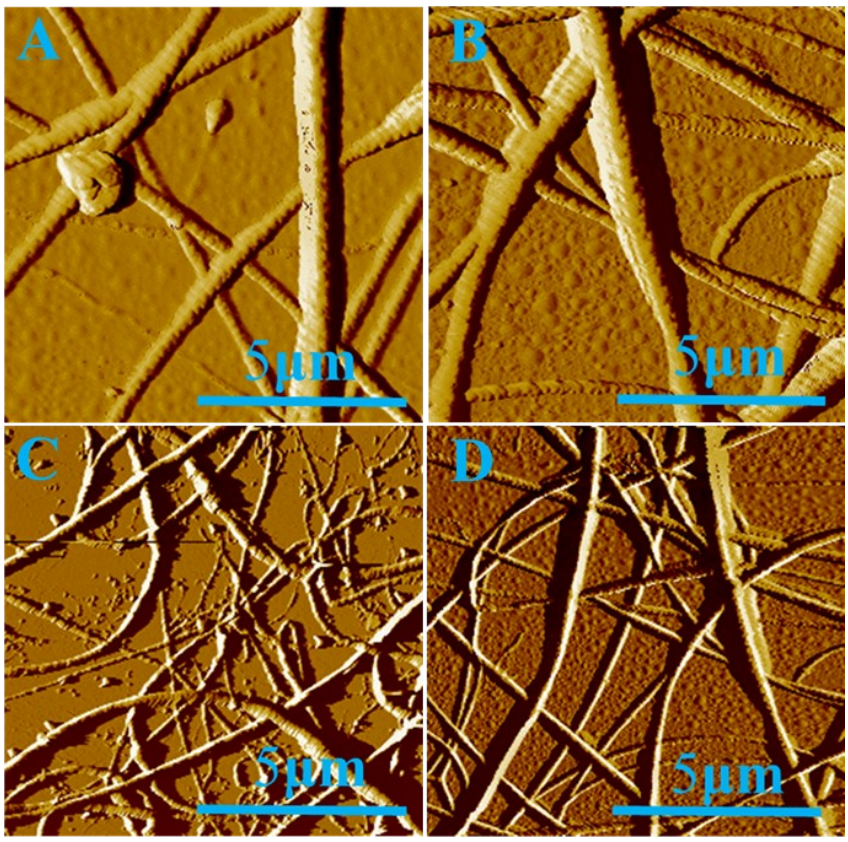


**Figure S8.** AFM topography images of electrospun fluorescence nanofiber collected from (A) PM-NFs, (B) PMDM-NFs, (C) PMHM-NFs, and (D) PMSO-NFs.

**8. Investigation of the fluorescent images of nanofibers**

The synthesized nanofibers were characterized using fluorescence microscopy with both green (EX560/AF55 nm, EM 645/AF75 nm) and blue (EX475/AF50 nm, EM535/AF45 nm) filter channels, due to the use of two labeling-specific functional groups of the fluorescent oxazolidine

dyes, each possessing distinct properties. For the dye-labeled nanofibers, the fluorescence oxazolidine dye was mixed with the polymer solution during the pre-electrospinning stage for 12 hours at room temperature. This process ensures that the dye is embedded within the nanofibers during their formation. Two key factors in the final composition of the fluorescent nanofibers are crucial. The functional groups of oxazolidine, which serves as the fluorescent dye, and the matrix in which it is embedded. The results indicated that donor groups, such as hydroxyl and amine played a crucial role in the dye's interaction with the nanofiber surface, affecting the distribution and optical properties of oxazolidine, particularly enhancing the fluorescence emission intensity. This detailed labeling approach facilitated a clear visualization of the nanofibers' structure and optical properties, which can carefully consider in this research, as shown in Figure S9. The second factor involves the matrix, which incorporates polar functional groups like amine, sulfonic acid, and hydroxyl. These groups facilitate effective interactions with the surrounding environment; for instance, they can transmit the pH environmental changes to the oxazolidine molecule. In fact, the polymeric matrix acts as a connecting bridge between the oxazolidine and environmental changes, fostering a synergistic interaction between these two components. The OX-OH and OX-NM fluorescence dyes, which contain hydroxyl and amine functional group, respectively, were applied to label the nanofibers, serving as indicators for detecting of food spoilage.

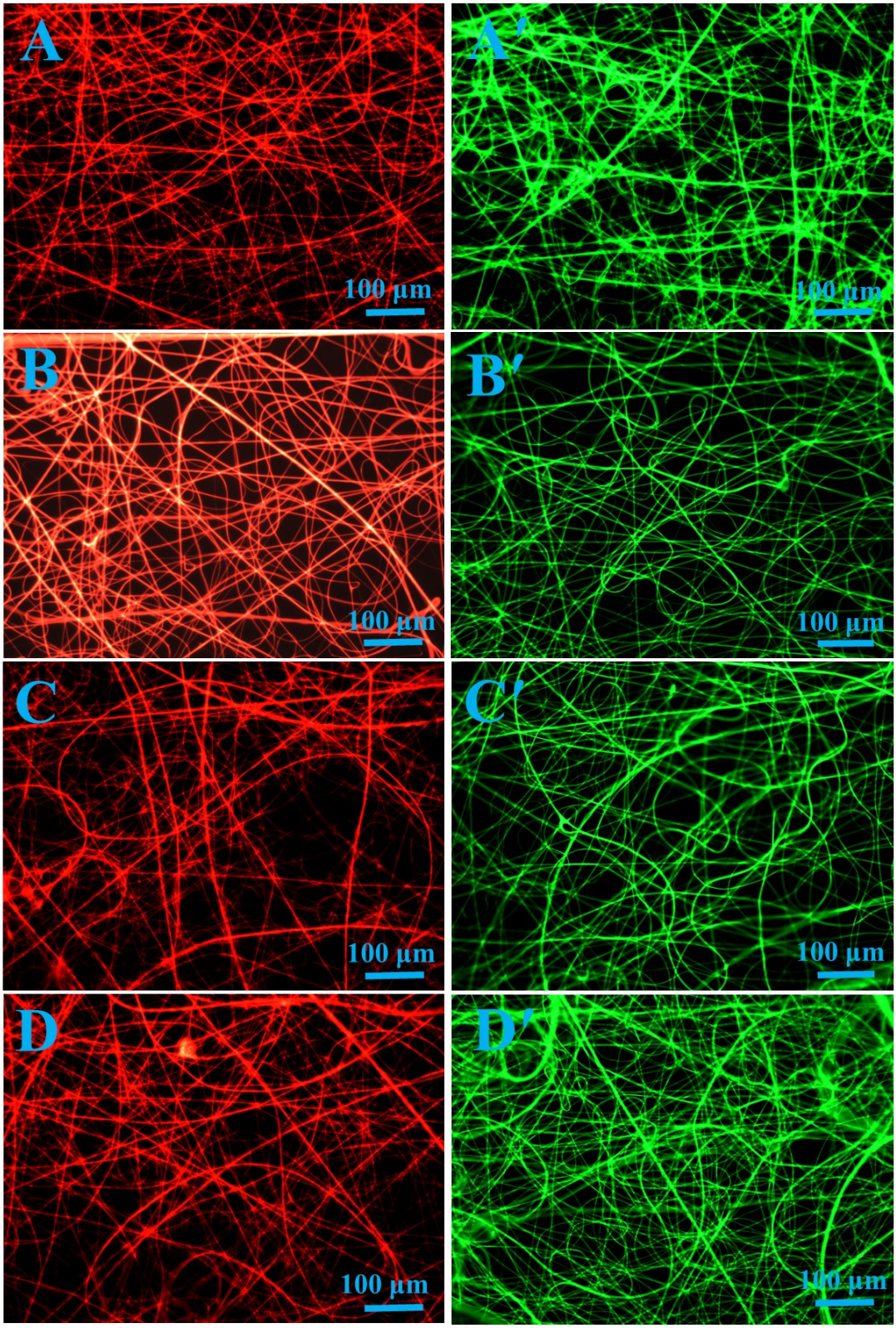
A
100 µm
A′
100 µm
B
100 µm
B′
100 µm
C
100 µm
C′
100 µm
D
100 µm
D′
100 µm

**Figure S9.** Fluorescence microscopy images of the electrospun nanofibers under UV irradiation prepared using (A, A′) PM-NFs, (B, B′) PMDM-NFs, (C, C′) PMHM-NFs, and (D, D′) PMSO-NFs, which (A–D) green filter doped with OX-NM dye, and (A′–D′) blue filter doped with OX-OH dye.

## 9. Evaluation the contact angle and three-dimensional surface roughness of the stimuli-chromic nanofibers

The chemical composition of a surface strongly influences its hydrophilicity and hydrophobicity. Surfaces composed of nanofiber with polar groups, such as hydroxyl, amine, and sulfonic acid groups, tend to exhibit hydrophilic properties. On the other hand, surface roughness can amplify the intrinsic hydrophilicity or hydrophobicity of a surface. The topography of the surface nanofibers is an important parameter for evaluating surface quality. A three-dimensional surface roughness was generated, as illustrated in Figure S10 (A′-D′). The relationship between contact angle and surface roughness is a key factor in understanding how liquids interact with solid surfaces. For hydrophilic surfaces, decreased roughness result in a decreased contact angle, while for hydrophobic surfaces, increased roughness leads to an increased the contact angle. Understanding this relationship is essential for designing materials with specific wetting properties. As shown in Figure S10 (A-D), the contact angle significantly decreases with the presence of hydrophilic groups. The PMSO-NFs, which contain a sulfonic acid functional group, exhibit the lowest contact angle of 55° and the least surface roughness of 0.0311μm. In contrast, the PMDM-NFs, and the PMHM-NFs samples, which contain amine and hydroxyl polar groups, have contact angles of 110° and 116° and surface roughness values of 0.458 μm and 0.268 μm, respectively.

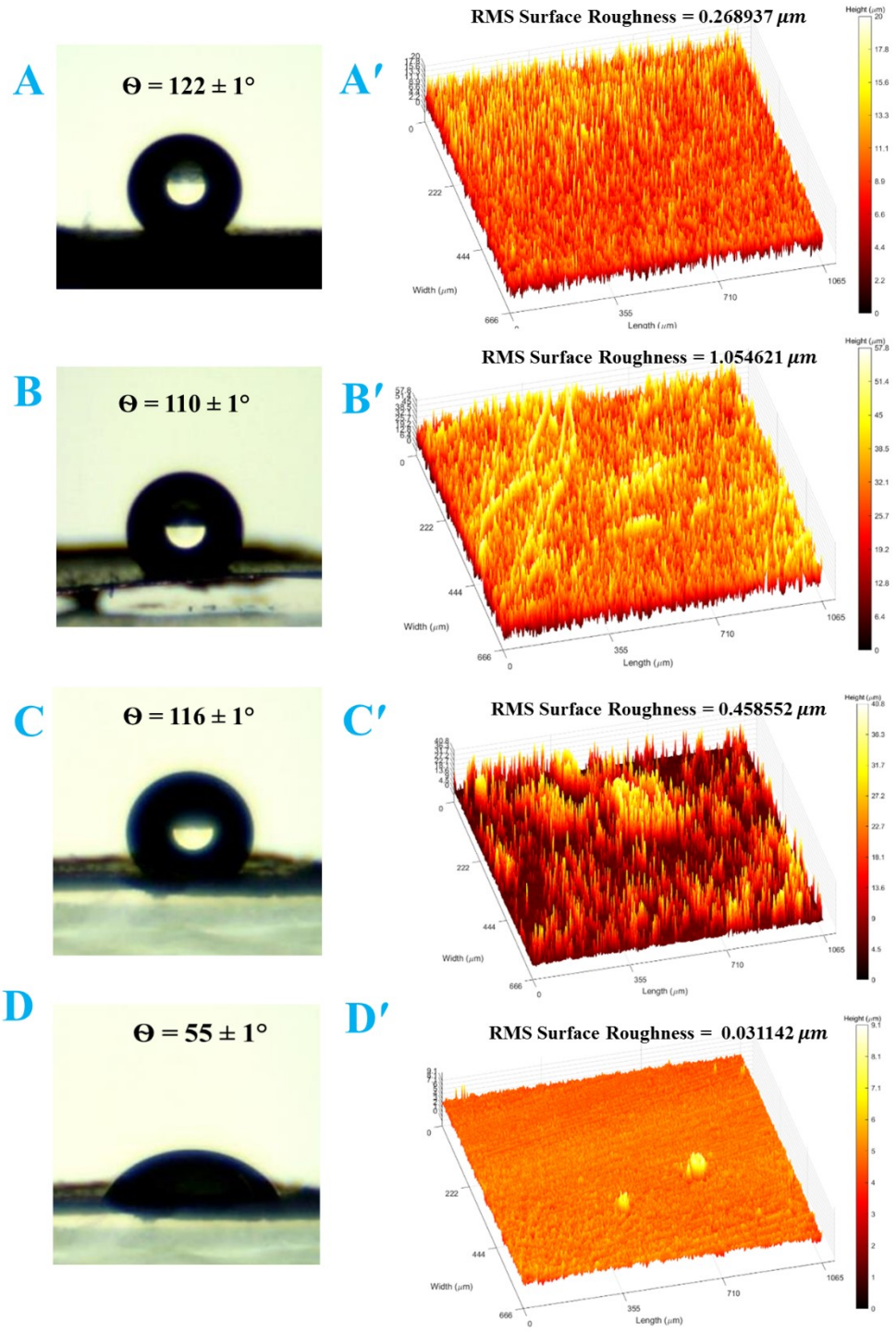
A
Θ = 122 ± 1°
A′
RMS Surface Roughness = 0.268937 μm
B
Θ = 110 ± 1°
B′
RMS Surface Roughness = 1.054621 μm
C
Θ = 116 ± 1°
C′
RMS Surface Roughness = 0.458552 μm
D
Θ = 55 ± 1°
D′
RMS Surface Roughness = 0.031142 μm
Width (μm)
Length (μm)
Height (μm)

**Figure S10.** Surface wettability (A-D) (contact angle of water droplet with a volume of 0.1 mL), and a three-dimensional rough surface (A′-D′) the nanofibrous (Root Mean Square (RMS). (A, A′) PM-NFs, (B, B′) PMDM-NFs, (C, C′) PMHM-NFs, and (D, D′) PMSO-NFs

## 10. The impact of local polarity on optical characteristics of oxazolidine derivatives

The variations in absorbance peaks and fluorescence intensities indicate the differing interactions between the functional groups on the copolymer nanofibers and the oxazolidine dye. As shown in Figures S11A, A′, the absorbance intensity and pattern for both OX-OH and OX-NM were affected by the polarity of the functional groups where the PMDM-NFs sample exhibited the lowest absorbance intensity among the other samples due to intramolecular proton exchange between the aromatic tertiary amine group and the aliphatic hydroxyl group within the oxazolidine ring. Also, the PMDM-NFs sample exhibited the highest fluorescence intensity in both OX-OH and OX-NM as shown in Figures S11 B, B′, while the fluorescence of other samples exhibited less dependence on the polarity of their functional groups. The pronounced fluorescence peak for the oxazolidine dye (OX-OH) within the PMDM-NFs matrix can likely be ascribed to proton exchange involving the aromatic hydroxyl group of OX-OH and the alkaline tertiary amine groups in the matrix. This interaction induces a negative charge on the phenolate oxygen of OX-OH, thereby enhancing its fluorescence intensity. In the PMDM-NFs(OX-NM) sample, a blue shift in the fluorescence spectrum (Figure S11B′) indicates a variation in the optical properties due to the deprotonation of the aliphatic hydroxyl group, leading to the formation of a closed oxazolidine structure as schematically illustrated in Scheme S2. For the PMSO-NFs(OX-NM) and PMSO-NFs(OX-OH) samples, strong ionic interactions of the sulfonic acid with tertiary amine and hydroxyl group, likely facilitated by proton and electron transfer mechanisms, resulted in a significant reduction in fluorescence intensity (Figure S11 B, B′). Overall, the observed fluorescence behaviors are

primarily influenced by the polarity of the media and the copolymer matrix, which are closely related to the solvatochromic phenomenon.

The fluorescence intensity results align accompanied by the color shifts observed in the CIE 1931 colorimetric diagram, as illustrated in Figures S11 C, C′. Specifically, the color of PMDM-NFs(OX-OH) shifted from yellow to pink under UV light irradiation (365 nm) more prominently than the other samples, due to the strong interactions between OX-OH and tertiary amine groups. In contrast, the other samples exhibited only subtle color shifts and maintained similar positions on the colorimetric diagram.

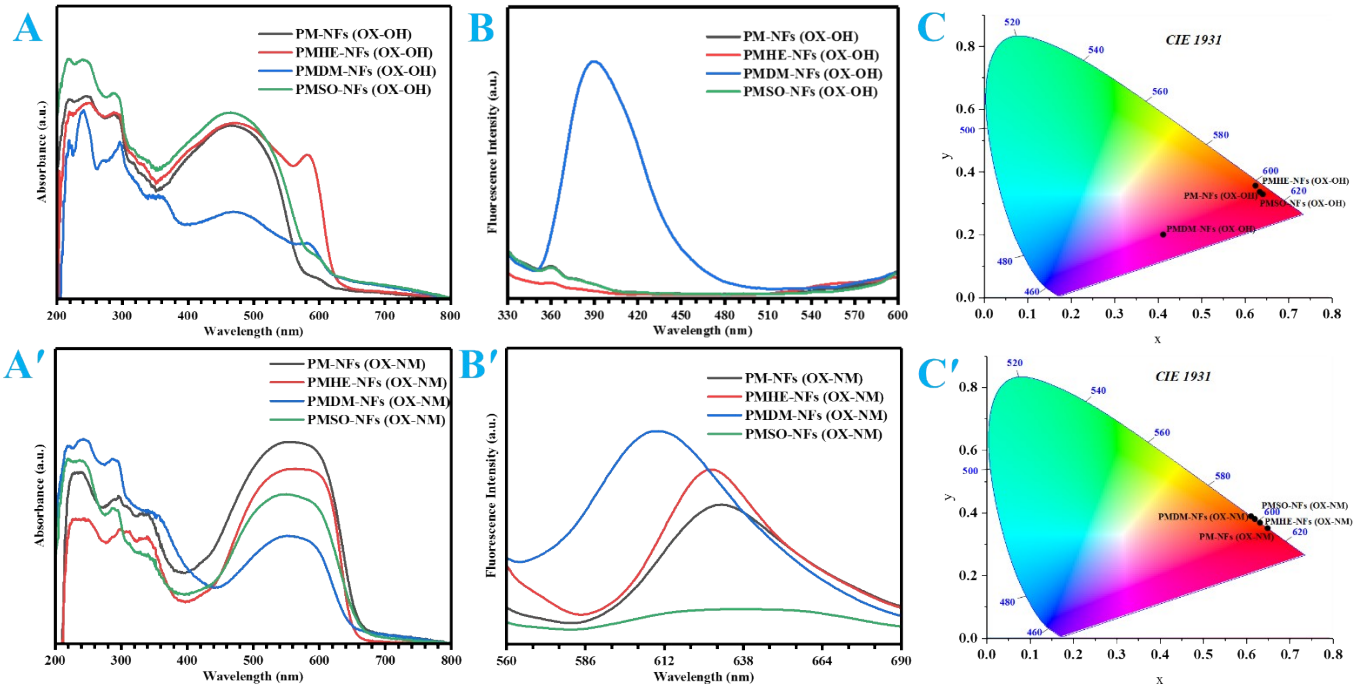


**Figure S11.** (A, A′) Solid UV−Vis, (B, B′) Solid fluorescence excited at 310 nm and 540 nm for OX-OH & OX-NM respectively, (C, C′) CIE colorimetric diagram of nanofibers

## 11. Isomerization of oxazolidine

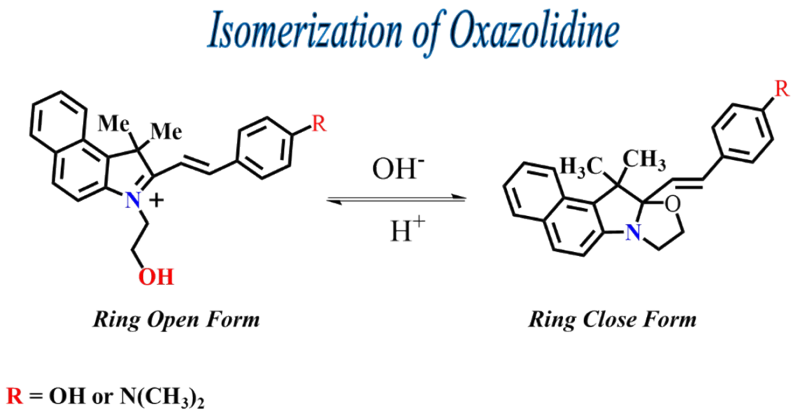


**Scheme S2.** Isomerization of Oxazolidine

## 12. pH responsivity of oxazolidine

Oxazolidine derivatives exhibit a pronounced pH-dependent response. In first step, we investigated the pH responsiveness on oxazolidine solutions due to the release of acidic and alkaline vapors during food spoilage process. In this way, an aqueous solution of OX-OH and OX-NM with a concentration of $10^{-5}$ M was prepared, and their pH responsiveness was examined by UV-Vis and fluorescence spectroscopy. As shown in Figure S12A, the absorbance intensity of the OX-OH solution was analyzed across a pH range of 1 to 14, through gradual increasing of solution's acidity. In acidic pH conditions, the hydroxyl groups in the structure of oxazolidine may undergo protonation. These structural changes could lead to an increase in light absorption in specific regions of the UV-Vis spectrum. Protonation may alter the energy levels of electronic transitions, thereby enhancing absorption at particular wavelengths. Additionally, the fluorescence intensity (Figure S12A′) decreased in basic media. Under basic pH conditions, the compound may undergo deprotonation, leading to a change in its molecular structure. These alterations can result in

decreased stability of the excited state and/or a reduction in the efficiency of energy transfer within the molecule. As a consequence, the compound may exhibit a diminished capacity for fluorescence, thereby leading to a drop in its fluorescence intensity. In the OX-NM solution (Figure S12B, B′) both UV-Vis and fluorescence spectra exhibit an increasing trend in both absorption intensity and fluorescence emission is observed at acidic pH, respectively. This is followed by a gradual decrease in intensity as the pH shifts toward basic conditions. This behavior in oxazolidine molecules containing amine groups is attributed to the protonation-deprotonation equilibrium of the amine groups. At acidic pH, the amine groups are protonated, which enhances both absorption and fluorescence emission. As the pH shifts towards basic conditions, the amine groups become deprotonated, leading to changes in the molecular structure or electronic properties in the manner that reduce the absorption and fluorescence intensity. The photographic images demonstrating the pH-responsivity of samples under Visible and UV light (at 254 nm) are presented in Figure S12.

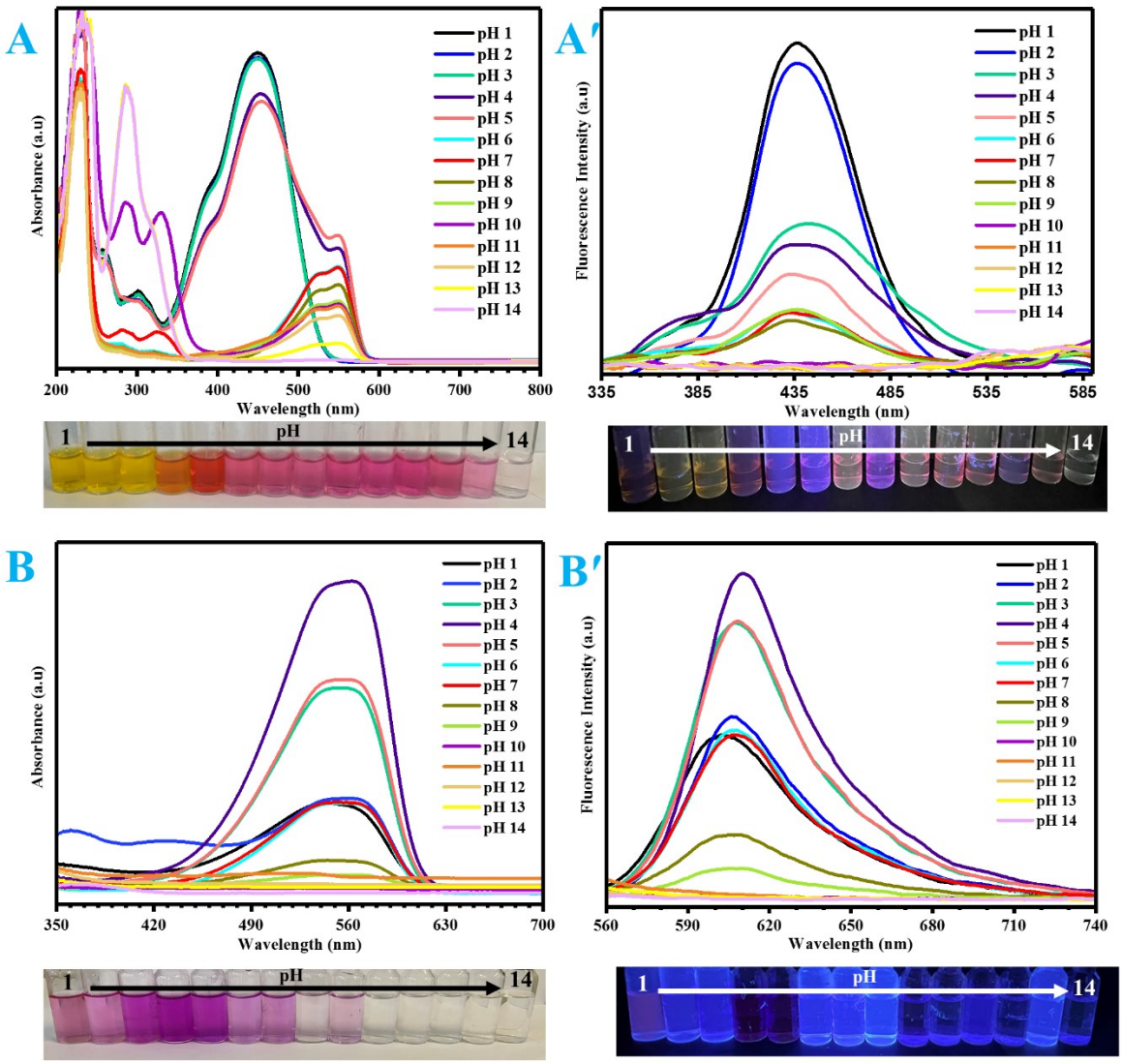


**Figure S12.** (A, B) UV−Vis, (A′, B′) fluorescence excited at 310 nm and 540 nm for OX-OH & OX-NM solution respectively in different pHs (1-14)

In the next stage, the pH responsiveness of nanofiber tags containing oxazolidine was investigated. As shown in Figure S13, all the smart tags exhibit excellent pH responsiveness in both acidic and basic media. As illustrated in Figure S13A, the absorbance intensity significantly decreased from pH 1 to pH 9 and gradually increased from pH 10 to pH 14. This behavior can be attributed to the transition of PDMAEMA from its hydrophilic to hydrophobic form, which is

due to the pH-dependent protonation and deprotonation of the amine groups in PDMAEMA, with the pKa of DMAEMA ranging from 7.5 to 8.5. At lower pH (acidic conditions), the hydroxyl groups are also protonated, resulting in a highly hydrophilic form. As the pH increases and surpasses the pKa, the hydroxyl groups become deprotonated, making the smart tags more hydrophobic. This transition from hydrophilic to hydrophobic form significantly affects the material's optical properties, including absorption and fluorescence behavior. The fluorescence intensity of PMDM-NFs (OX-NM) in Figure S13A′ follows a similar trend to that of the absorbance intensity. The PMDM-NFs (OX-OH) tag demonstrates good pH responsivity, as shown in Figure S13 B, B′ due to protonation and deprotonation of PDMAEMA. As illustrated in Figure S13C, C′ the absorption patterns observed for $SO_3$ differ from those of DMAEMA, which can be attributed to the interaction between the functional groups of the matrix and oxazolidine. This suggests that the polar groups of the matrix significantly influence the oxazolidine structure.

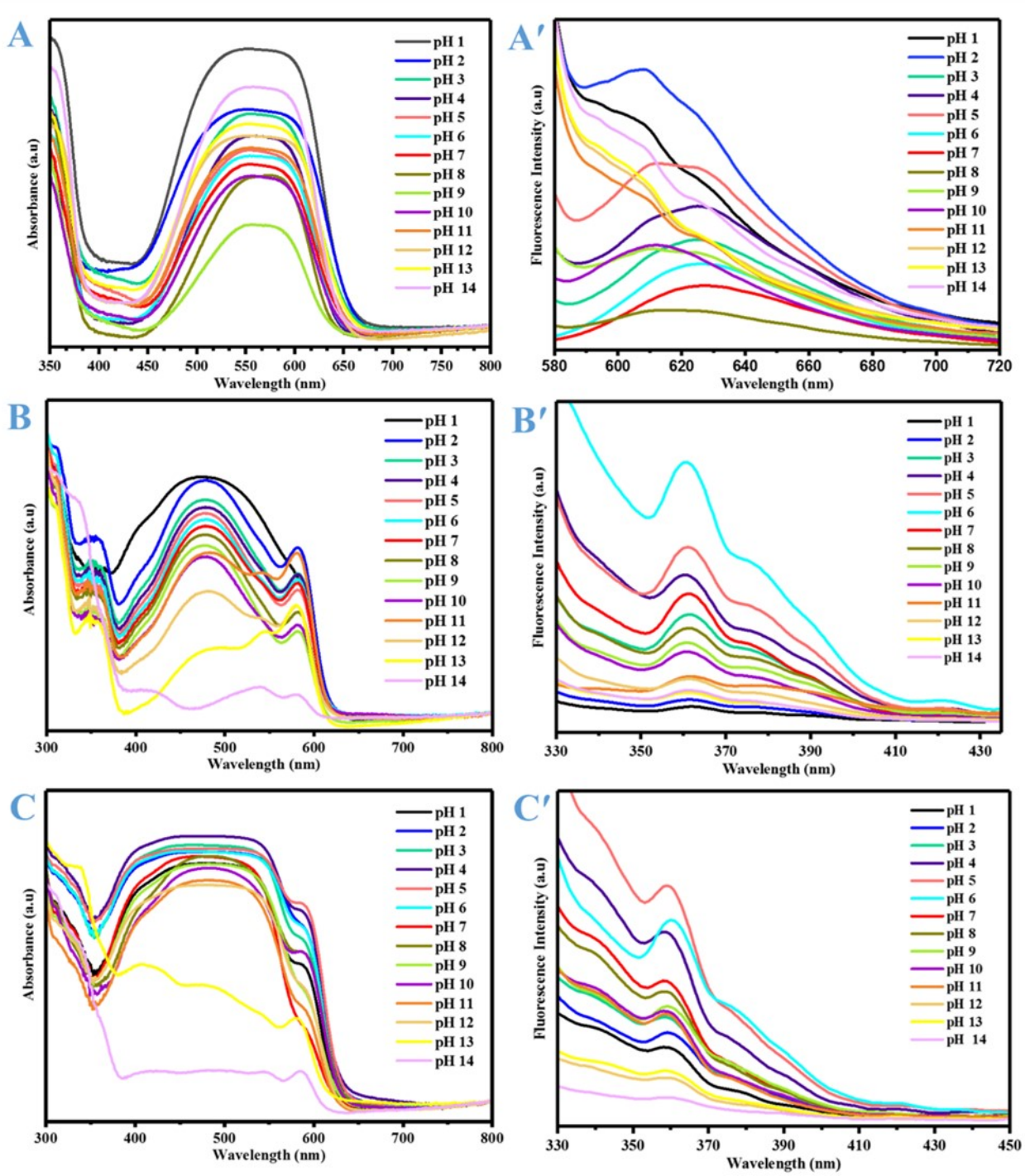


**Figure S13.** Solid-state (A, B, C) UV−Vis, and (A′, B′, C′) fluorescence excited at 310 nm and 540 nm for PMDM-NFs (OX-NM), PMDM-NFs (OX-OH), and PMSO-NFs (OX-OH) tags respectively in different pHs (1-14)

**13. Amine responsivity of oxazolidine**

Some foods, such as fish, produced the alkaline vapors (amine products), Therefore, we investigated the amine-responsivity of oxazolidine derivatives solution in response to both aliphatic and aromatic amines. The fluorescence response of these molecules to amines can be influenced by several factors, including the electronic structure of the molecule, the nature of the amine (whether aromatic or aliphatic), and environmental conditions (such as solvent polarity, temperature, and pH). The effect of on amines on the fluorescence properties of a molecule depends on their interaction with the excited and ground states of the fluorophore. Consequently, solutions of OX-NM and OX-OH each at a concentration of $10^{-5}$ M, were prepared in (1:1, v/v) mixture of acetone and acetonitrile, in the presence of various amines (also at a concentration of $10^{-5}$ M). Their amine responsivity was then investigated using UV-Vis and fluorescence spectroscopy. According to Figure S14, the OX-NM solution exhibits remarkable amine-responsiveness compare to OX-OH. The key difference between aromatic and aliphatic amines in the context of oxazolidine derivatives lies in the conjugative interactions and the stabilization of the excited state. Aromatic amines, with their ability to extend conjugation and delocalize electron density, stabilize the excited state more effectively, resulting in higher fluorescence intensity and stronger UV-Vis absorption. In contrast, aliphatic amines, which lack such conjugative interactions, are less capable of stabilizing the excited state, leading to lower fluorescence intensity and weaker UV-Vis absorption. However, when an oxazolidine containing a hydroxyl functional group is present, it may somewhat disrupt this conjugation. While the hydroxyl group donates electron density, it may also reduce the conjugation efficiency, resulting in lower overall stabilization of the excited state. As mentioned later in this article, labels containing OX-NM can serve as more effective indicators for detecting fish spoilage than other

types of labels. Additionally, the photographic images of OX-OH and OX-NM solutions in response to a variety of aliphatic and aromatic amines under UV light and visible light are presented in Figure S15.

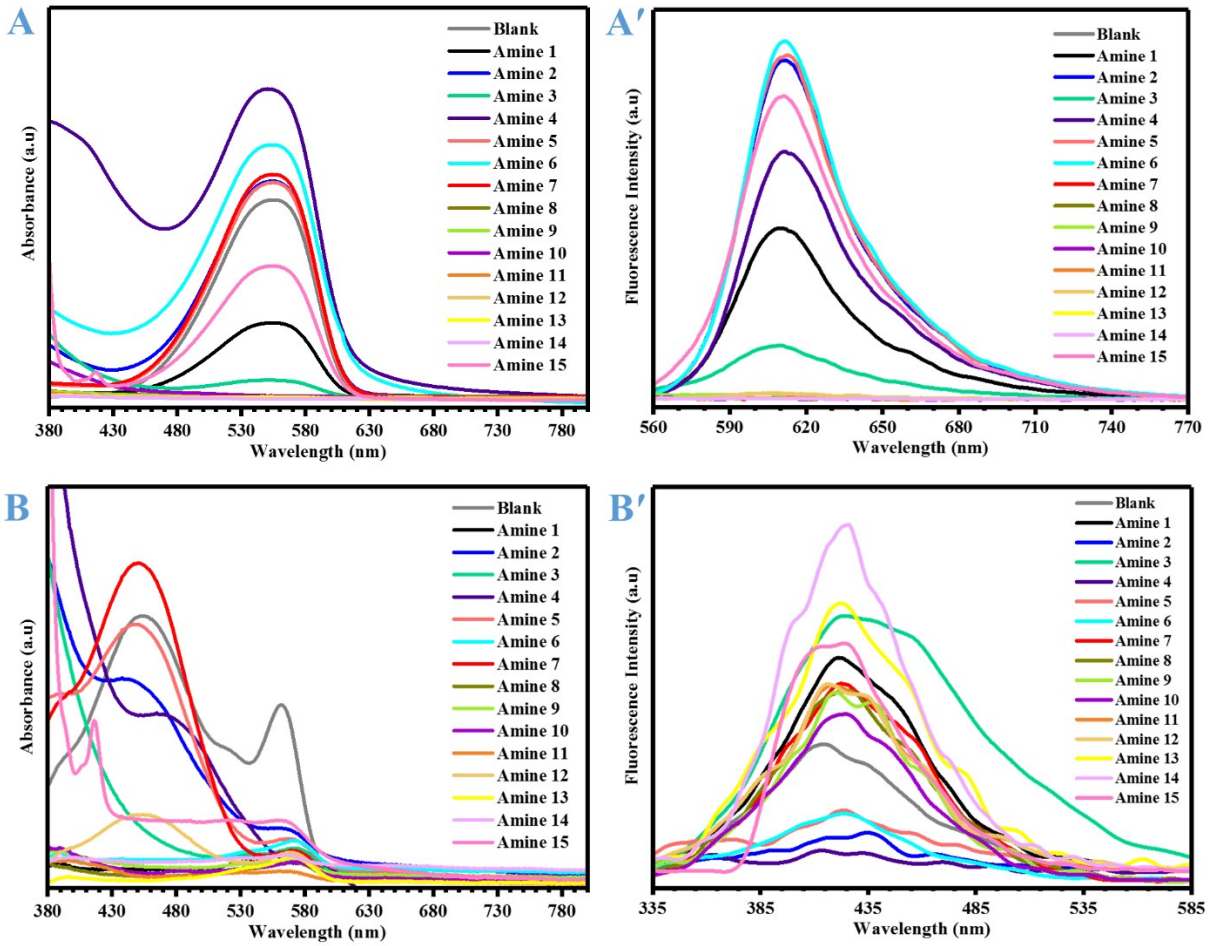


**Figure S14.** (A, B) UV−Vis, (A′, B′) fluorescence excited at 310 nm and 540 nm for OX-NM and OX-OH solution respectively in different Amines (1: hydroxylamine, 2: 2-Amino-4-methylphenol, 3: Benzylamine, 4: p-Anisidine, 5: p-Toluidine, 6: N-methylaniline, 7: Methylamine, 8: Triethylamine, 9: Butylamine, 10: Diethylamine, 11: Tribenzylamine, 12: Benzylamine, 13: Tris(2-aminoethyl) amine, 14: 1-Naphthylamine, 15: Ethylenediaminetetraacetic acid)

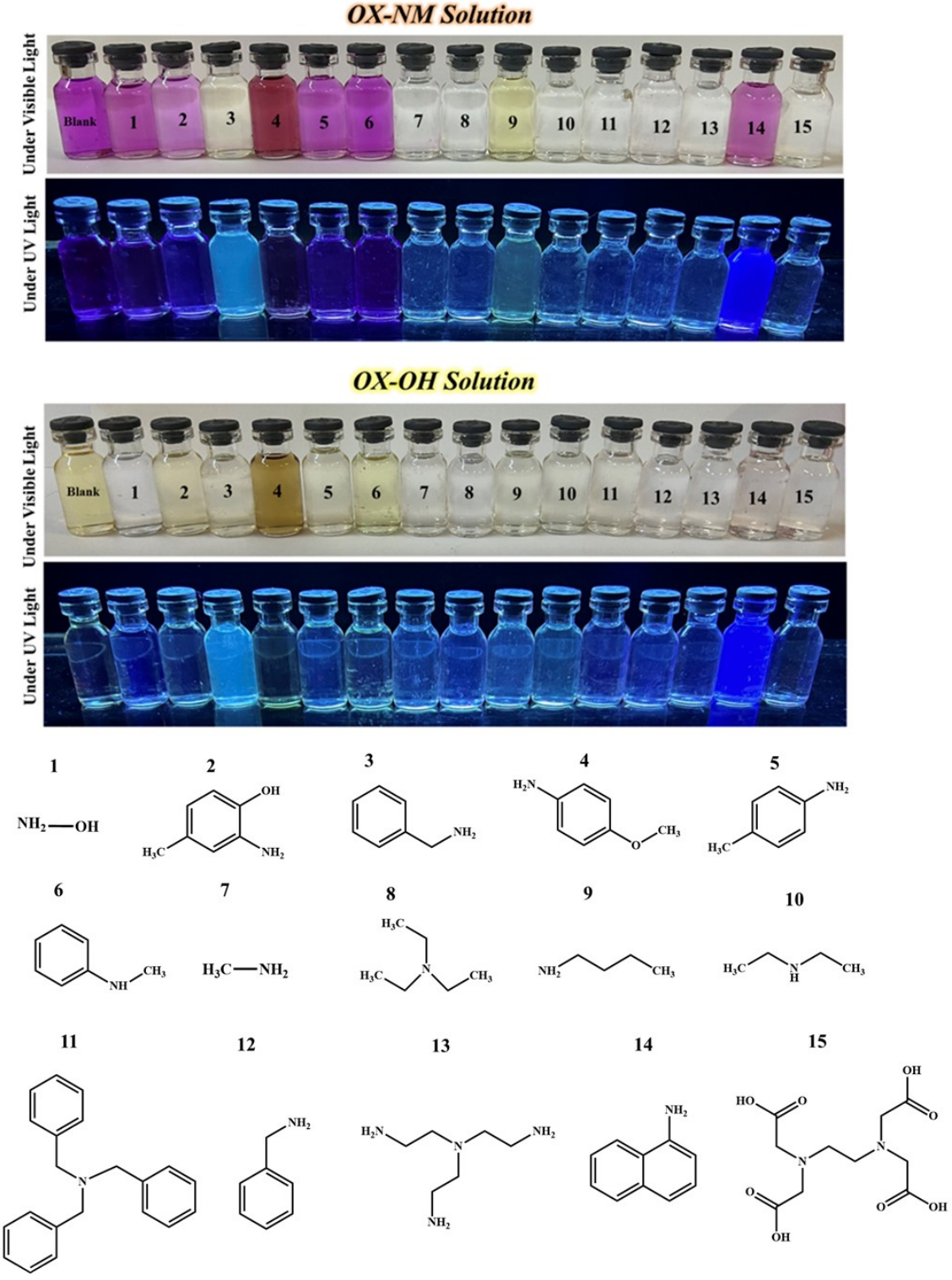


**Figure S15.** Amine responsivity of OX-NM and OX-OH solution under UV light and Visible light (at 254 nm) toward aliphatic and aromatic ones.

## 14. Investigation the stokes shift

The Stokes shift is defined as the difference between the wavelengths at which the absorption "$\lambda_{max(abs)}$" and emission spectra "$\lambda_{max(abs)}$" reach their maximum peaks for the same electronic transition. The results indicate that the solvatochromic behavior of OX-OH and OX-NM is influenced by the polarity of functional groups within the nanofibers and the surrounding medium (acidic or basic), due to hydrogen bonding interactions between these functional groups and the oxazolidine molecules. This is evident from changes in the Stokes shift, as well as in the UV-Vis and fluorescence spectra. The PMSO-NFs(OX-OH) in basic condition, PMDM-NFs(OX-OH) in acidic condition, and PMDM-NFs(OX-NM) in both acidic and basic conditions were found to be the best candidate for application in the final intelligent tag for food spoilage detection. As instance, in basic media, the sulfonic acid functional group of PMSO-NFs(OX-OH) is deprotonated, creating a negative charge that results in the increased fluorescence intensity. In acidic conditions, tertiary amine functional group is protonated and cannot interact with oxazolidine molecules, leading to fluorescence quenching, and we did not observe a stokes shift. The details of the results are presented in Table S3.

**Table S3.** Spectroscopic parameters extracted from UV-Vis and fluorescence spectra

| Sample | Absorbance ($^{1}\lambda_{max(abs)}$, nm) | Emission ($^{2}\lambda_{max(em)}$,nm) | Stokes Shift (nm) |
|---|---|---|---|
| PM-NFs (OX-OH) | 471 | 360 | 111 |
| PM-NFs (OX-OH) + $NH_3$ | 581 | 362 | 219 |
| PM-NFs (OX-OH) + HCl | 470 | 360 | 110 |
| PMDM-NFs(OX-OH) | 474 | 390 | 84 |
| PMDM-NFs (OX-OH) + $NH_3$ | 581 | 392 | 189 |
| PMDM-NFs (OX-OH) + HCl | 474 | No Emission | - |
| PMHM-NFs (OX-OH) | 473 | 360 | 113 |
| PMHM-NFs (OX-OH) + $NH_3$ | 581 | 389 | 192 |
| PMHM-NFs (OX-OH) + HCl | 471 | 360 | 111 |
| PMSO-NFs (OX-OH) | 466 | 360 | 106 |
| PMSO-NFs (OX-OH) + $NH_3$ | 537 | 391 | 146 |
| PMSO-NFs (OX-OH) + HCl | 470 | 360 | 110 |
| PM-NFs (OX-NM) | 568 | 631 | 63 |
| PM-NFs (OX-NM) + $NH_3$ | 567 | 635 | 68 |
| PM-NFs (OX-NM) + HCl | 568 | No Emission | - |

| | | | |
|---|---|---|---|
| **PMDM-NFs(OX-NM)** | **564** | **610** | **46** |
| **PMDM-NFs (OX-NM) + $NH_3$** | **356** | **600** | **244** |
| **PMDM-NFs (OX-NM) + HCl** | **470** | **617** | **147** |
| **PMHM-NFs (OX-NM)** | **475** | **626** | **151** |
| **PMHM-NFs (OX-NM) + $NH_3$** | **472** | **612** | **140** |
| **PMHM-NFs (OX-NM) + HCl** | **578** | **631** | **53** |
| **PMSO-NFs (OX-NM)** | **467** | **630** | **163** |
| **PMSO-NFs (OX-NM) + $NH_3$** | **538** | **621** | **83** |
| **PMSO-NFs (OX-NM) + HCl** | **472** | **632** | **160** |

[1]: $\lambda_{max(abs)}$ is the maximum absorbance wavelength in UV-Vis spectra collected from Figure 2, 3 (A, B, C, D)

[2]: $\lambda_{max(em)}$ is the maximum emission wavelength in fluorescence spectra collected from Figure 2, 3 (A′, B′, C′, D′)

## 15. Investigation of the reusability of halochromic nanofibers

After investigation the optical properties of nanofibers, three types of nanofiber tags were selected: PMSO-NFs(OX-OH) for use in in basic conditions, PMDM-NFs(OX-OH) for acidic conditions, and PMDM-NFs(OX-NM) for both acidic and basic environments. These photoluminescence nanofibers serve as intelligent tags for detecting food spoilage, which is indicated by the acidic or alkaline volatile compounds produced by bacterial decomposition and oxidation processes associated with food spoilage. Therefore, the reversibility of the pH-responsiveness of the intelligent nanofibers was examined using solid UV-Vis spectroscopy. This analysis aimed to

develop a photoluminescent pH-responsive nanofiber indicators for real-time visual monitoring of food spoilage within the industry. One of the novel interesting features of these tags is their reusability and reversibility, allowing them to be employed multiple times without any drop in optical properties. As shown in Figure S15, the tags underwent multiple cycles of acid or base treatment, with each sample being subjected to a specific pH that elicited the optimal response. The nanofibers resist degradation from exposure to various chemicals vapors such as acids, and bases which is the another innovative aspect of this project. When used as nanofibers as tags, the optical properties remain even after multiple uses, consistently detecting minor pH changes that indicate spoilage. However, in the case of small molecule oxazolidine without a polymer carrier, a significantly poor optical properties were observed. The pH-sensitive functional groups on the nanofibers remain active and effective despite repeated exposure to fluctuating pH levels. Based on the results from of UV-Vis and fluorescence spectroscopy (Figure S15B, B′), the PMDM-NFs(OX-NM) demonstrates responsiveness in both acidic and basic media, confirming its successful reusability in both environments. Additionally, Movie 3 demonstrates the reusability and reversibility of halochromic nanofiber sample when exposed to ammonia vapors.

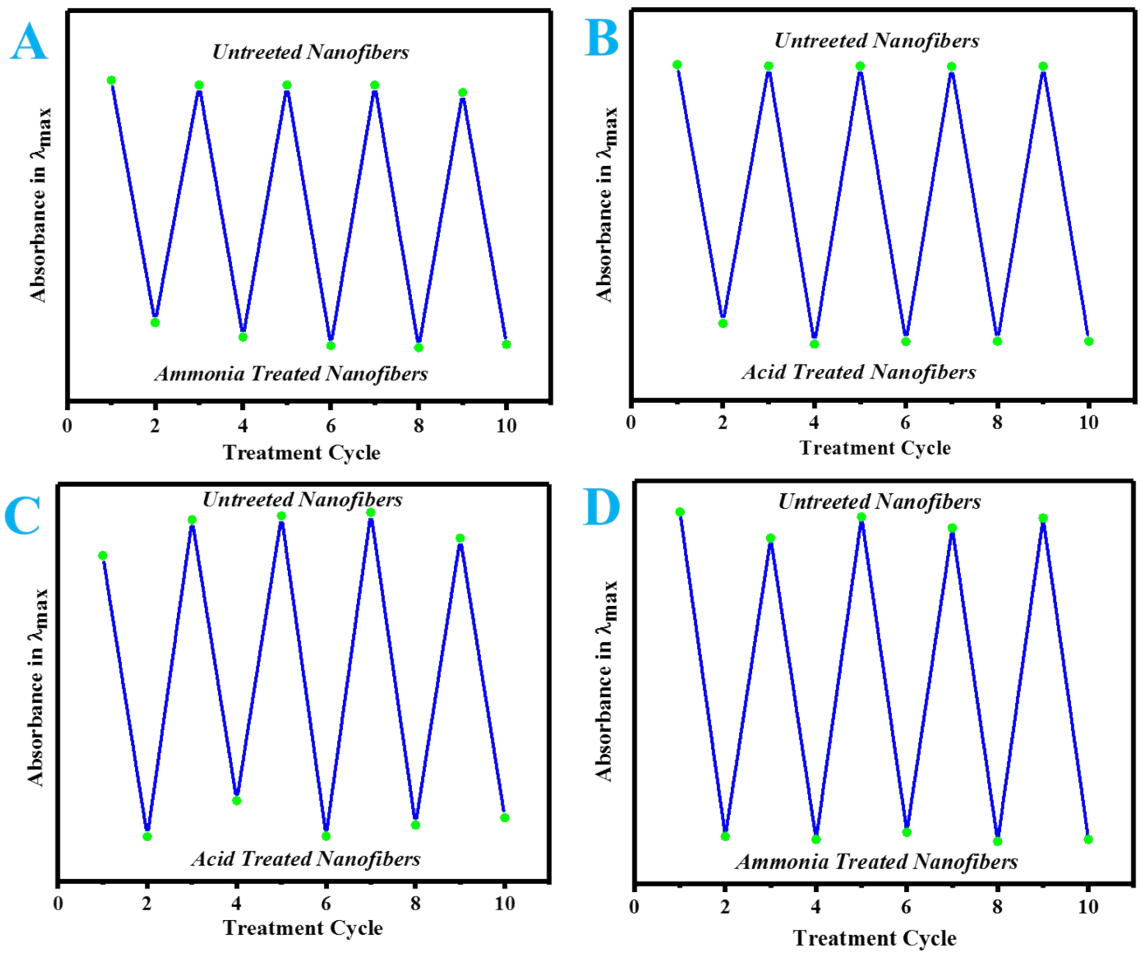


**Figure S16.** Investigation the reusability of halochromic nanofibers by solid UV-Vis with acidic and basic treatment. (A) PMSO-NFs(OX-OH), (B) PMDM-NFs(OX-OH), (C& D) PMDM-NFs(OX-NM)

## 16. Investigation of the kinetics of pH changes as a function of time for detection of milk spoilage

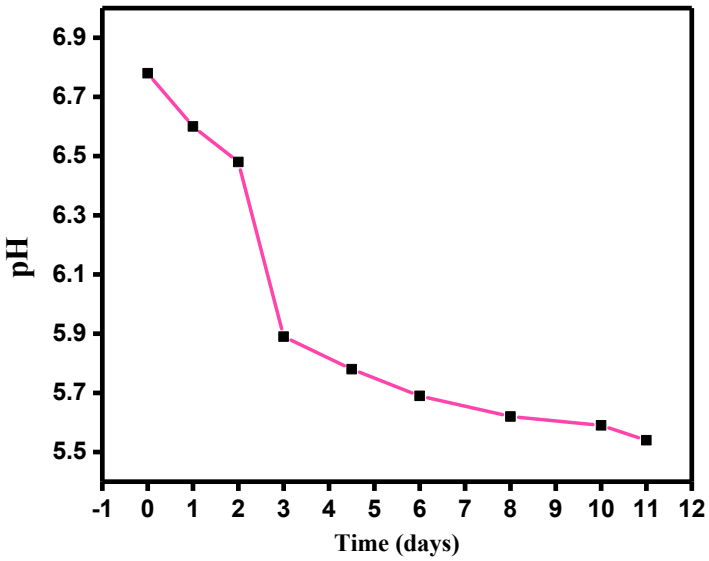


**Figure S17.** Monitoring of pH changes as a function of time for detection of spoilage of pasteurized milk with UV-Vis spectroscopy